Sedimentology (2004) **51,** 127–144 doi: 10.1046/j.1365-3091.2003.00615.x

Diagenetic overprinting of the sphaerosiderite palaeoclimate proxy: are records of pedogenic groundwater $\delta^{18}O$ values preserved?

DAVID F. UFNAR*, LUIS A. GONZÁLEZ†‡, GREG A. LUDVIGSON‡§¶, ROBERT L. BRENNER¶ and BRIAN J. WITZKE§¶
**Department of Geology, University of Southern Mississippi, Hattiesburg, MS 39406, USA (E-mail: David.Ufnar@usm.edu)*
†Department of Geology, University of Kansas, 1475 Jayhawk Blvd, Room 120, Lawrence, KS 66045-7613, USA
‡Center for Global and Regional Environmental Research, University of Iowa, Iowa City, IA 52242, USA
§Iowa Geological Survey Bureau, Iowa City, IA 52242, USA
¶Department of Geoscience, 121 TH, University of Iowa, Iowa City, IA 52242-1379, USA

ABSTRACT

Meteoric sphaerosiderite lines (MSLs), defined by invariant $\delta^{18}O$ and variable $\delta^{13}C$ values, are obtained from ancient wetland palaeosol sphaerosiderites (millimetre-scale $FeCO_3$ nodules), and are a stable isotope proxy record of terrestrial meteoric isotopic compositions. The palaeoclimatic utility of sphaerosiderite has been well tested; however, diagenetically altered horizons that do not yield simple MSLs have been encountered. Well-preserved sphaerosiderites typically exhibit smooth exteriors, spherulitic crystalline microstructures and relatively pure (> 95 mol% $FeCO_3$) compositions. Diagenetically altered sphaerosiderites typically exhibit corroded margins, replacement textures and increased crystal lattice substitution of Ca^{2+}, Mg^{2+} and Mn^{2+} for Fe^{2+}. Examples of diagenetically altered Cretaceous sphaerosiderite-bearing palaeosols from the Dakota Formation (Kansas), the Swan River Formation (Saskatchewan) and the Success S2 Formation (Saskatchewan) were examined in this study to determine the extent to which original, early diagenetic $\delta^{18}O$ and $\delta^{13}C$ values are preserved. All three units contain poikilotopic calcite cements with significantly different $\delta^{18}O$ and $\delta^{13}C$ values from the co-occurring sphaerosiderites. The complete isolation of all carbonate phases is necessary to ensure that inadvertent physical mixing does not affect the isotopic analyses. The Dakota and Swan River samples ultimately yield distinct MSLs for the sphaerosiderites, and MCLs (meteoric calcite lines) for the calcite cements. The Success S2 sample yields a covariant $\delta^{18}O$ vs. $\delta^{13}C$ trend resulting from precipitation in pore fluids that were mixtures between meteoric and modified marine phreatic waters. The calcite cements in the Success S2 Formation yield meteoric $\delta^{18}O$ and $\delta^{13}C$ values. A stable isotope mass balance model was used to produce hyperbolic fluid mixing trends between meteoric and modified marine end-member compositions. Modelled hyperbolic fluid mixing curves for the Success S2 Formation suggest precipitation from fluids that were < 25% sea water.

Keywords Cretaceous, diagenesis, isotopes, palaeoclimatology, palaeosols sphaerosiderite.

INTRODUCTION

Sphaerosiderites are millimetre-scale $FeCO_3$ spherulites that form in wetland soil environments (Stoops, 1983; Landuydt, 1990). Sphaerosiderites are an important geochemical archive of 'greenhouse-world' palaeohydrological information (Ludvigson *et al.*, 1998) and have been used to improve our understanding of mid-Cretaceous (Albian) humid continental palaeoenvironments (e.g. Ufnar *et al.*, 2001, 2002; White *et al.*, 2001). Isotopic compositions obtained from Cretaceous sphaerosiderites commonly reveal diagenetic trends with invariant $\delta^{18}O$ values and highly variable $\delta^{13}C$ values. These trends have been used to define meteoric sphaerosiderite lines (MSLs; Ludvigson *et al.*, 1998). The MSLs indicate that the sphaerosiderites preserve an oxygen isotope record of precipitation in shallow, early diagenetic meteoric phreatic fluids, thus providing a proxy for Cretaceous precipitation (Ludvigson *et al.*, 1998).

University of Iowa workers have analysed over 100 sphaerosiderite-bearing palaeosols throughout the Cretaceous Western Interior Foreland Basin, and the MSLs have served as the basis for interpreting palaeohydrology during the mid-Cretaceous of the Western Interior Basin (Ludvigson *et al.*, 1998; White *et al.*, 2000a, 2001; Ufnar *et al.*, 2002). However, not all sphaerosiderite-bearing horizons yield isotopic compositions defining pure MSLs. Indeed, in a relatively significant number of sphaerosiderite-bearing horizons, sphaerosiderite minor element chemistries suggest that sphaerosiderites developed in slightly brackish systems resulting from physical mixing of sea water and meteoric water. Sphaerosiderites that precipitated from mixed fluids may yield hyperbolic $\delta^{18}O$ vs. $\delta^{13}C$ compositional trends that are tangential to MSLs (Ludvigson *et al.*, 2000).

Although siderite is a relatively insoluble carbonate mineral, diagenetically overprinted sphaerosiderites have been encountered, and the isotopic compositions obtained from such units do not always generate MSLs (White *et al.*, 2000b), nor do they define fluid mixing trends. Such samples cannot be presumed to retain primary geochemical records without closer examination. Well-preserved sphaerosiderites have smooth margins (often with euhedral crystal terminations) and exhibit radial concentric crystalline microstructures. Diagenetically altered sphaerosiderites may exhibit features such as chemically corroded margins, pyrite replacement textures and/or coarsely crystalline 'sparry' siderite or unit crystal textures. Palaeosols exhibiting altered sphaerosiderites commonly contain calcite cements.

Here, altered sphaerosiderite-bearing units from the Dakota Formation of Kansas, the Swan River Formation and Success S2 Formation of Saskatchewan are interpreted, and an attempt is made to resolve the diagenetic history. A primary focus of this work is to isolate all diagenetic carbonate phases, determine their isotopic compositions and evaluate the preservation of original sphaerosiderite $\delta^{18}O$ values. From several case examples, it can be shown that texturally and compositionally altered sphaerosiderites may preserve early diagenetic isotopic compositions, and can serve as a proxy for meteoric water compositions. However, without careful identification of all carbonate phases and their isolation for sampling, it is very easy inadvertently to obtain homogenized data from multiple phases that might lead to erroneous interpretations. These sphaerosiderite-bearing palaeosols are an important terrestrial palaeoclimatic proxy and may also mark the position of stratigraphically significant horizons (i.e. sequence and parasequence boundaries).

METHODS

Lithological descriptions and samples were collected from the Kansas Geological Survey (KGS) Jones #1 Core (NE, NE, NE Sec. 2, T. 10S, R. 8W, Lincoln County, KS, USA), the Saskatchewan Geological Survey (SGS) Yarbo #17S core; 1-24-20-33W1, Saskatchewan, and the Shell Mayberries core 16-4-6-5w4 stored at the Geological Survey of Canada Core facility in Calgary, Alberta (Fig. 1). The specimens analysed in this study are small (centimetre-scale) 'plugs' recovered from the cores and will be referred to as the core depth interval (metres below surface) from which they were obtained.

Carbonate diagenesis was evaluated using light microscopy, cathodoluminescence (CL), epifluorescence petrography and scanning electron microscopy (SEM). Polished slabs from each of the palaeosol horizons were microsampled using a microscope-mounted drill assembly with a 0·5 mm tungsten carbide burr. All samples extracted for mass spectrometry were analysed at the University of Iowa Paul H. Nelson Stable Isotope Laboratory. To ensure against calcite contamination, the siderite sample powders were treated with dilute acetic acid before roasting.

Powdered samples were roasted *in vacuo* at 380 °C to remove volatile contaminants. Samples

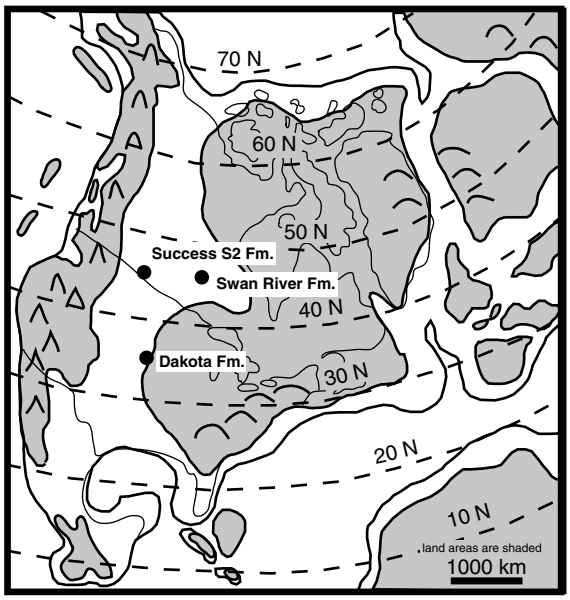

Fig. 1. Mid-Cretaceous palaeogeographic reconstruction of N. America illustrating the studied palaeosol locations (modified from Scotese, 1991).

were then reacted with anhydrous phosphoric acid at 75 °C in a Kiel III automated carbonate reaction device coupled to the inlet of a Finnigan MAT 252 isotope ratio mass spectrometer. All isotope ratios are reported relative to the Vienna PeeDee Belemnite (VPDB) standard, with analytical precision of better than ±0·1‰ $\delta^{13}C$ and $\delta^{18}O$ values. Siderite data were corrected with the experimentally determined temperature-dependent oxygen isotope fractionation factor of Carothers *et al.* (1988).

Electron microprobe analyses were conducted on sphaerosiderites and calcite cements from the three different units using a Jeol JXA-8900R electron microprobe at the University of Minnesota, Minneapolis, MN, USA. Siderite analyses were performed simultaneously using wavelength dispersive spectrometry at an accelerating voltage of 15 kV, a beam current of 10 nA and a beam diameter of 5 μm. The following X-ray lines and standards were measured (simultaneously): $Ca_{K\alpha 1}$ (calcite), $Mg_{K\alpha 1}$ (dolomite), $Mn_{K\alpha 1}$ (rhodonite), $Fe_{K\alpha 1}$ (siderite) and $Sr_{K\alpha 1}$ (strontianite).

RESULTS

General lithostratigraphy

The Late Albian (Witzke *et al.*, 1996a) Dakota Formation of north-eastern Kansas, south-eastern Nebraska and western Iowa is generally characterized by fluvial sandstones, pedogenically altered overbank mudstones, carbonaceous shales, lignites and tidally influenced mudstones and siltstones (Joeckel, 1987; Macfarlane & Hamilton, 1990; Hamilton, 1994; Macfarlane *et al.*, 1994; Witzke & Ludvigson, 1994; Witzke *et al.*, 1996a,b; Brenner *et al.*, 2000). The 85–95 m depth interval of the Dakota Formation in the KGS Jones #1 core is characterized by deeply weathered, plinthic palaeosols composed of mottled very pale orange (10YR 8/2), moderate red brown (10R 4/6) and light brown (5YR 5/6) silty mudstones (Fig. 2). The matrix is interlaced with numerous calcite-filled soil macropores that are visible as white streaks on the core surface (Fig. 3). The calcite-filling macropores produced a rigid framework about which other soil components were probably deformed during burial compaction. The Early Late Albian Swan River Formation of south-eastern Saskatchewan (Playford, 1971; McNeil & Caldwell, 1981) generally consists of a basal sandy fluvial unit and an upper shale-dominated marine unit (Price, 1963; White *et al.*, 2000b). The 400·85–400·95 m depth interval of the SGS Yarbo core is characterized by pedogenically altered fluvial sandstones, floodplain mudstones and carbonaceous shales (Fig. 2). The Success S2 Formation of south-western Saskatchewan has been interpreted as Hauterivian(?) to Aptian(?) and is characterized by fluvial channel-fill sandstones and fine-grained overbank deposits (Leckie *et al.*, 1995, 1997). The upper portion of the Success S2 Formation in the 16-4-6-5w4 (Shell Mayberries) core consists of pedogenically altered, kaolinitic sandstones with an abundance of sphaerosiderites, root traces, organic matter, pyrite and clay coatings (Leckie *et al.*, 1997) (Fig. 2). Lithological features are illustrated in Figs 4 and 5, and descriptions of the sampled palaeosols are summarized in Table 1.

Dakota Formation Jones core (87·8–87·9 m)

Isotopic analyses. The $\delta^{18}O_{VPDB}$ values of sphaerosiderite nodules in the 87·8–87·9 m depth interval of the KGS Jones core range between −6·05‰ and −4·51‰ (SD ±0·43‰), and the $\delta^{13}C_{VPDB}$ values of the sphaerosiderites range between −23·05‰ and −19·02‰ (SD ±1·50‰). The sphaerosiderite values yield an MSL with an average $\delta^{18}O_{VPDB}$ value of −5·27‰ (Fig. 6). The poikilotopic calcite cements have more depleted oxygen isotopic values than the sphaerosiderites. The $\delta^{18}O_{VPDB}$ values of the calcite cements range

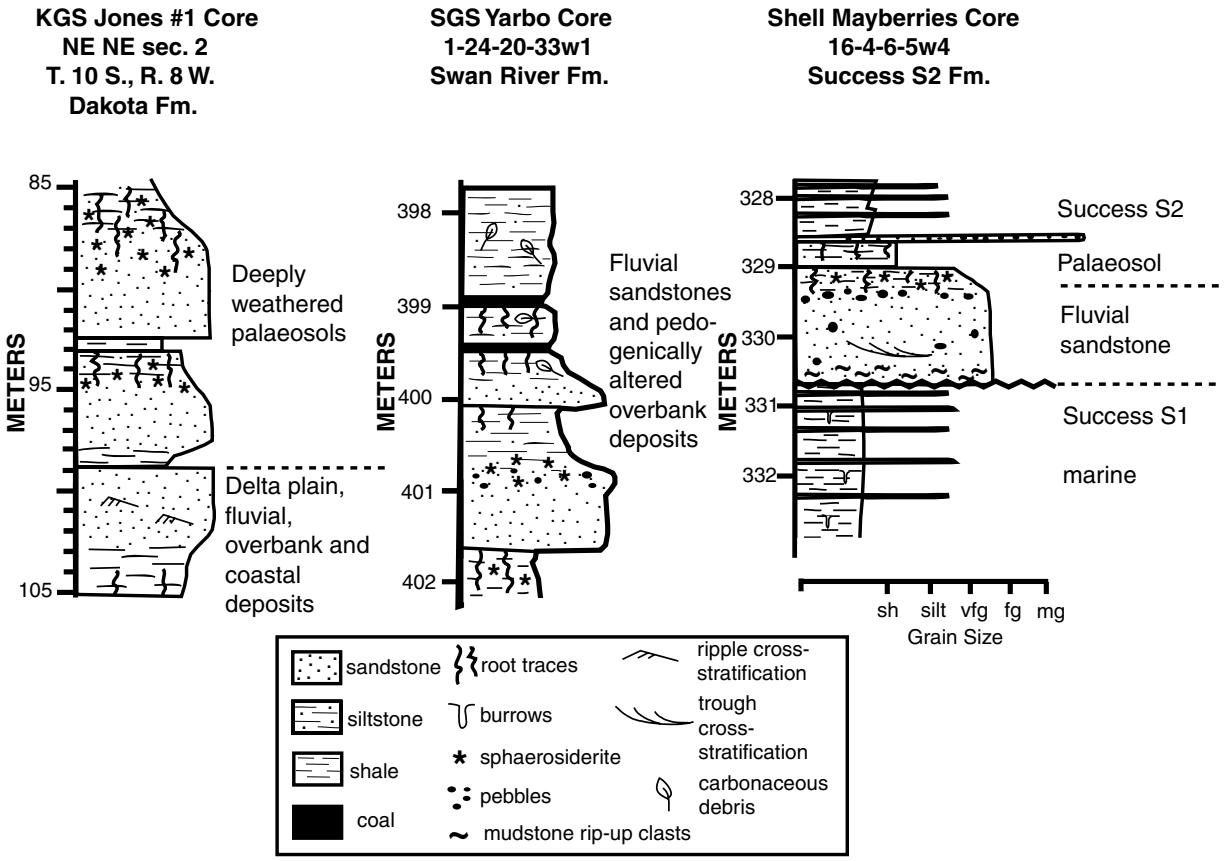

Fig. 2. Generalized lithostratigraphic logs from the KGS Jones core (Dakota Formation), the SGS Yarbo core (Swan River Formation) and the Shell Mayberries core (Success S2 Formation).

between −8·29‰ and −7·28‰ (SD ±0·36‰). The $\delta^{13}C_{VPDB}$ values of the calcite cements range between −19·50‰ and −17·26‰ (SD ±0·85‰). The calcite cement values yield a meteoric calcite line (MCL) with an average $\delta^{18}O$ value of −7·81‰ (Fig. 6).

Microprobe analyses. Transects across altered sphaerosiderites from this interval show significant variations in the mol% $FeCO_3$ (Fig. 7). The sphaerosiderite cores generally consist of 88·35–99·38 mol% $FeCO_3$, with minor enrichments in Ca, Mg, Mn and Sr (Fig. 7). Substitutions of Ca in the nodule cores range from 0·11 to 3·88 mol% $CaCO_3$, Mg ranges from 0·15 to 7·91 mol% $MgCO_3$, Mn ranges from 0·26 to 2·25 mol% $MnCO_3$ and Sr does not exceed 0·014 mol% $SrCO_3$. Peaks in Mg and Ca substitutions occur along the margins of nodules where substitutions reach 20–22 mol% $MgCO_3$ and 6–10 mol% $CaCO_3$ respectively (Fig. 8). Manganese substitution in the margins is generally < 2 mol% $MnCO_3$, and the Sr concentrations were generally very low, not in excess of 1·0 mol% $SrCO_3$. Comparison of Mg/Fe and Mg/(Ca+Mg) ratios shows significant variations even in the siderite nodule cores. The core Mg/Fe ratios range from 0·0016 to 0·091, and the Mg/(Ca+Mg) ratios range from 0·47 to 0·88.

The calcite cements have variable compositions, ranging from 86 to 97 mol% $CaCO_3$. The pure $CaCO_3$ end-members have minor enrichments in Mn (≈ 0·5 mol% $MnCO_3$) and Fe (up to 1·5 mol% $FeCO_3$). The impure $CaCO_3$ has significant enrichments in Fe (5·5–6·5 mol% $FeCO_3$) and Mg (3·0–7·0 mol% $MgCO_3$). The Sr concentrations range from trace amounts up to 2 mol% $SrCO_3$. A microprobe transect of several points across a siderite nodule exhibits peaks in Fe (mol%) near the core that degrade towards the nodule margin where Ca (mol%) increases into the matrix (Fig. 9).

Swan River Formation (400·85–400·95 m)

Isotopic analyses. The $\delta^{18}O_{VPDB}$ composition of sphaerosiderite nodules in the 400·85–400·95 m depth interval of the Saskatchewan Geological Survey Yarbo Core ranges between −6·26‰ and

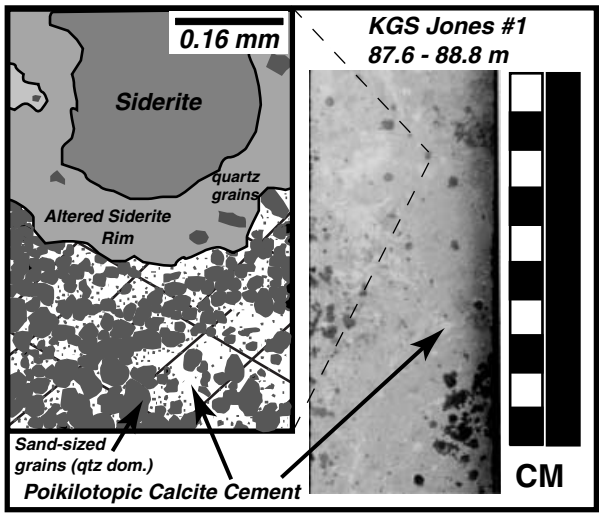

Fig. 3. The photograph shows the appearance of the sampled Dakota Formation palaeosol (87·6–88·8 m) on the sawed split core surface (KGS Jones #1). The white streaks are calcite cement-filled palaeosol macropores. The illustration is a sketch of a photomicrograph from ≈88 m depth in the Jones #1 core. The illustration is intended to show the geometry of the poikilotopic calcite cement-filled pores at the microscopic scale (cross-hatched pattern). Note that the illustration does not exactly match the core surface (where indicated with the dashed lines) because the thin section was cut from the opposite split section of core.

−5·00‰ (SD ±0·49‰), and the $\delta^{13}C_{VPDB}$ values of the sphaerosiderites range between −6·65‰ and −6·04‰ (SD ±0·20‰). The sphaerosiderite values yield an MSL with an average $\delta^{18}O_{VPDB}$ value of −5·5‰ (Fig. 6). The poikilotopic calcite cements have more depleted isotopic values than the sphaerosiderites. The $\delta^{18}O_{VPDB}$ values of the calcite cement range between −12·58‰ and −12·33‰ (SD ±0·09‰), and the $\delta^{13}C_{VPDB}$ values of the calcite cements range from −27·00‰ to −25·71‰ (SD ±0·53‰). The calcite cement values yield a meteoric calcite line (MCL) with a mean $\delta^{18}O_{VPDB}$ value of −12·44‰ (Fig. 6).

Microprobe analyses. The sphaerosiderites in the Swan River Formation of the Yarbo Core are relatively pure ranging from 95·8 to 97·8 mol% $FeCO_3$ (Fig. 7). The nodules have minor substitutions of calcium, with 0·91–2·83 mol% $CaCO_3$. Substitutions of Mn and Mg range from 0·35 to 1·18 mol% $MnCO_3$, and 0·49 to 0·95 mol% $MgCO_3$ (Fig. 8). Nodules have trace substitutions of Sr not exceeding 0·025 mol% $SrCO_3$. The Mg/Fe ratios range from 0·0050 to 0·0098, and the Mg/(Ca+Mg) ratios range from 0·18 to 0·37.

The calcite cement is 93·2–95·0 mol% $CaCO_3$ and has minor amounts of Fe, Mg and Mn (Fig. 7). Minor element substitutions range from 2·14 to 2·29 mol% $FeCO_3$, 1·40 to 2·24 mol% $MgCO_3$ and 1·70 to 2·40 mol% $MnCO_3$. Minor substitutions of Sr range from 0·09 to 0·10 mol% $SrCO_3$.

Success S2 Formation, Mannville Group (329·0–329·25 m)

Isotopic analyses. The siderite nodule components are too small to sample individually (see descriptions in Table 1). Thus, the isotopic analyses discussed below represent homogenized samples obtained from the cores and margins of the nodules. The $\delta^{18}O_{VPDB}$ values of sphaerosiderite nodules in the 329·0–329·25 m depth interval of the 16-4-6-5w4 (Shell Mayberries) core range between −8·68‰ and −6·63‰ (SD ±0·56‰), and the $\delta^{13}C_{VPDB}$ values of the sphaerosiderites range between −0·78‰ and +1·72‰ (SD ±0·81‰). The sphaerosiderites yield an average $\delta^{18}O_{VPDB}$ value of −7·62‰ (Fig. 6). There is a positive covariant trend between the $\delta^{18}O$ and $\delta^{13}C$ values for the Success S2 sphaerosiderites.

The poikilotopic calcite cements have more depleted isotopic values than the sphaerosiderites. The $\delta^{18}O_{VPDB}$ values of the two analyses of the calcite cement range between −13·03‰ and −12·64‰, and the $\delta^{13}C_{VPDB}$ values of the calcite cement range between −12·38‰ and −11·99‰ (Fig. 6).

Microprobe analyses. The sphaerosiderites in the Success S2 Formation have somewhat variable compositions that range from 88·33 to 95·42 mol% $FeCO_3$ (Fig. 7). Nodules have minor substitutions of Ca, Mn and Mg. Calcium substitutions range from 2·50 to 9·85 mol% $CaCO_3$, and Mn substitutions range from 1·00 to 2·90 mol% $MnCO_3$. The Mg substitutions range from 0·70 to 1·50 mol% $MgCO_3$, and Sr substitutions are not in excess of 0·06 mol% $SrCO_3$ (Fig. 8). The minor element substitutions are greatest in the nodule margins, and analyses of the vein-filling siderite show some significant increases in Ca (up to 9·85 mol% $CaCO_3$). The Mg/Fe ratios in the sphaerosiderites range from 0.0037 to 0·021, and the Mg/(Ca+Mg) ratios range from 0·113 to 0·41.

The calcite cement is 95·2–96·4 mol% $CaCO_3$ and has minor substitutions of Fe, Mg and Mn (Fig. 7). Substitution of Fe ranges from 2·15 to 2·87 mol% $FeCO_3$, Mg ranges from 0·81 to 1·28 mol% $MgCO_3$, and Mn ranges from 0·54 to 0·60 mol% $MnCO_3$. Substitutions of Sr are very low, not in excess of 0·15 mol% $SrCO_3$.

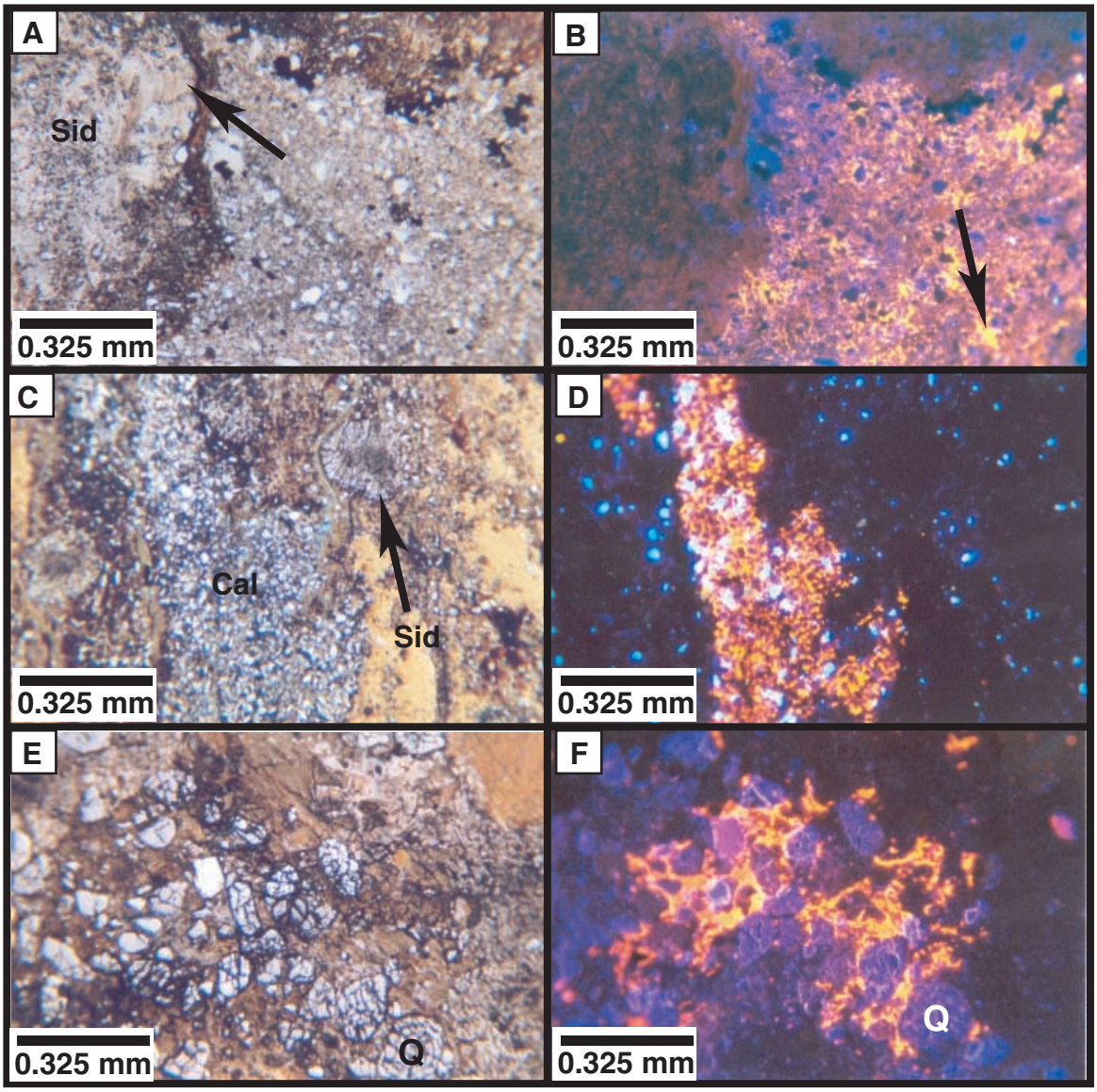

Fig. 4. (A) Plane light photomicrograph of the Dakota Formation sample showing a siderite nodule (Sid) with partial preservation of original concentric fabric (arrow) and the calcite-cemented matrix. (B) Cathodoluminescence (CL) photomicrograph of the same field-of-view in (A). The arrow points to a larger pore filled with orange luminescent calcite on the margins and bright yellow luminescent calcite in the pore centre. (C) Plane light photomicrograph of the Swan River Formation showing a sphaerosiderite nodule (arrow labelled Sid) and silt-rich calcite-cemented domain (Cal). (D) CL photomicrograph of the Swan River Formation field-of-view shown in (C) showing the uniform, bright orange luminescent poikilotopic calcite cement. (E) Plane light photomicrograph of the Success S2 Formation showing the quartz (Q) sand-rich matrix. (F) CL photomicrograph of the field-of-view shown in (E) shows the patchy distribution of calcite cement in the matrix. Note that the image is shifted slightly, so use the quartz grains labelled Q in each photomicrograph as a reference point. All the photomicrographs were taken at the same magnification, and the horizontal distance across each is 1·3 mm.

Groundwater compositions

The $\delta^{18}O$ values of sphaerosiderites and calcite cements are a proxy record of the groundwater compositions from which they precipitated. Using MSLs and MCLs extracted from individual palaeosol units and the temperature-dependent fractionation factors for siderite and calcite (Friedman & O'Neil, 1977; Carothers *et al.*, 1988), groundwater compositions were calculated over a range of temperatures (0–30 °C). From the empirical palaeotemperature data (Spicer & Corfield, 1992), a narrow range of groundwater compositions was determined for the

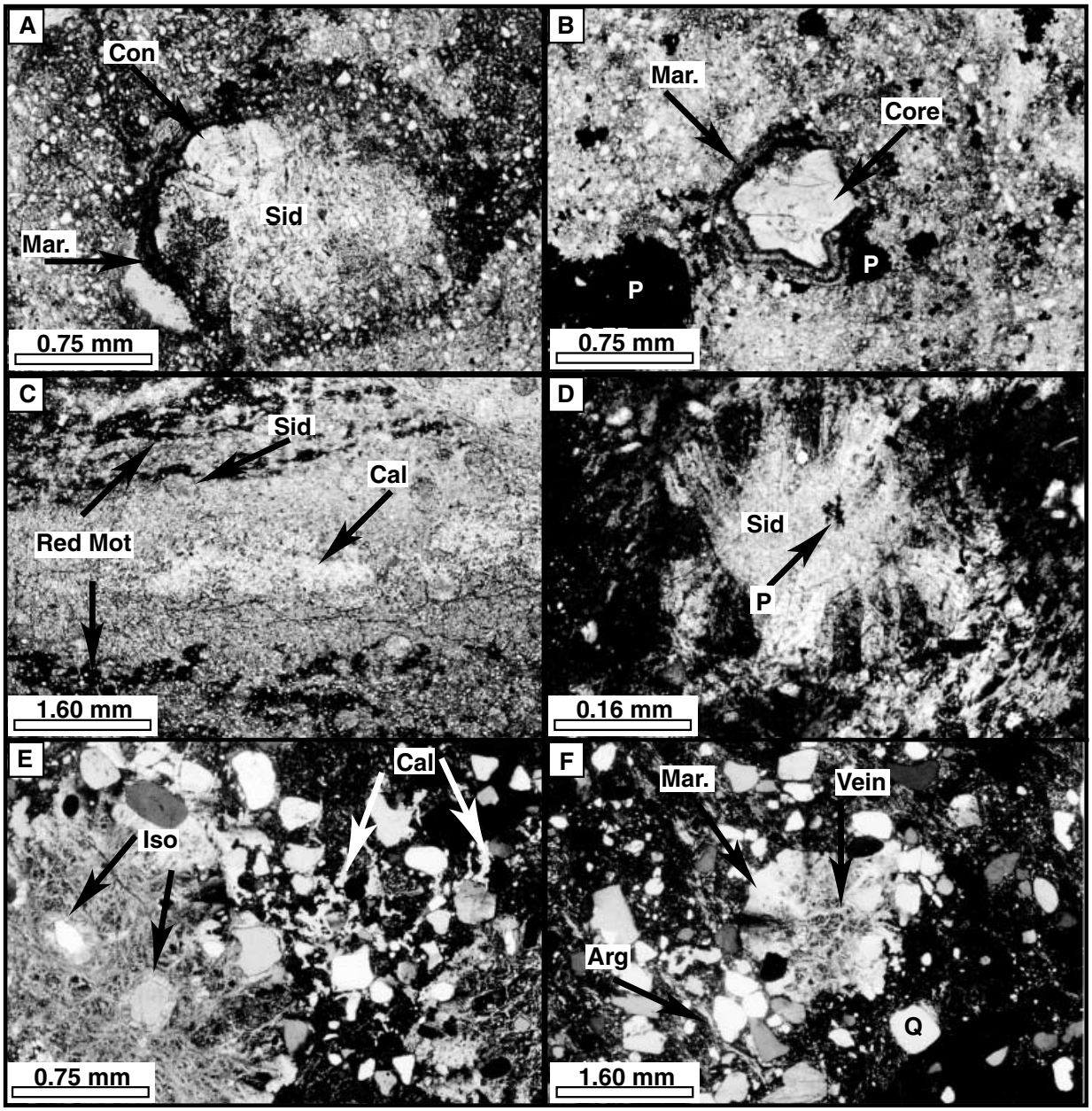

Fig. 5. (A) Siderite nodule of the Dakota Formation sample exhibiting preserved concentric crystalline microstructure (arrow labelled Con). The arrow labelled Mar points to the orange-brown, fibrous-textured nodule margin. The light grey domains in the matrix (surrounding white quartz grains) are the calcite cement (plane polarized light). (B) Siderite in the Dakota Formation sample that was reorganized to a unit crystal in the nodule core (arrow labelled Core). The exterior of the nodule (arrow labelled Mar) has two concentric layers of orange-brown, fibrous, impure siderite. (C) Plane polarized light view of the Swan River Formation matrix fabric showing the red-mottled domains (arrows labelled Red Mot), sphaerosiderites (sid) and the calcite-cemented domains (Cal). (D) Cross-polarized light photomicrograph of a sphaerosiderite in the Swan River Formation sample. The arrow labelled P points to cubic aggregate pyrite inclusions. Note the pseudo-uniaxial cross-extinction pattern (darkened domains) visible in the outer portion of the nodule. (E) Cross-polarized light view of Success S2 Formation siderite nodule with internal isopachous siderite cement (Iso) coatings on quartz sand grain inclusions. Also labelled are some patches of calcite (white arrows labelled Cal) cement in the matrix. (F) Siderite nodule of the Success S2 Formation showing the siderite-filled veins labelled Vein, and radial-concentric crystalline microstructure (Mar) on the margin of the nodule (cross-polarized light). The arrow labelled Arg points to a kaolinitic argillan.

Table 1. Lithological and pedogenic descriptions for the Dakota, Swan River and Success S2 Formation palaeosols analysed in this study.

Palaeosol	Lithology	Pedofeatures	Sphaerosiderites	Cements
Dakota Formation (KGS Jones core) 87·8–87·9 m depth interval	A quartzose siltstone, on a polished slabbed surface, this interval is faintly mottled with vertical to subvertical domains of greyish orange pink (10R8/2) and moderate orange pink (10R7/4) colouring. The matrix is dominated by subangular to subrounded quartz grains and rare micas engulfed in a ubiquitous, poikilotopic calcite cement.	Coatings are generally absent with the exception of some rare, thin ($\approx$ 50 μm thick), discontinuous, fragmented argillaceous coatings, exhibiting first-order birefringence and diffuse extinction patterns. Pyrite is very abundant and generally occurs as small aggregates of micron-scale cubes (each cubic form is $<$10 μm) or framboids disseminated throughout the matrix or as very large aggregates (2–3 mm diameter) that occupy voids formed through sphaerosiderite dissolution. The spherical shape of the pyrite aggregates (nodules) suggests replacement of sphaerosiderite, which is also indicated by the presence of relict inclusions of siderite.	The siderite nodules are large (0·5–2·5 mm in diameter) and generally lack a radial-concentric (spherulitic) crystalline microstructure. The cores of many nodules were recrystallized to unit crystals of siderite or to equant, blocky or 'sparry' siderite. Typically, the altered siderite cores are inclusion rich; however, some are clear and exhibit rhombohedral cleavage patterns. Rarely, original spherulitic fabrics were partially preserved through fabric-retentive neomorphic replacement. This is indicated by a partial loss of epifluorescent concentric zones. The siderite nodule margins are darker (5YR 5/6 – light brown) than the cores (10YR 6/2 – pale yellowish brown) and exhibit a radial fibrous microstructure. Typically, the boundary between the siderite cores and the outer radial-fibrous rims is marked by moderate brown (5YR 3/4) oxidation rings or quasicoatings (coatings related to the surfaces of grains or aggregates but not immediately adjoining them; Bullock *et al.*, 1985). The radial fibrous margins of the nodules commonly exhibit multiple moderate brown quasicoatings, and a few nodules contain some concentric dissolution voids. Many of the siderite nodules exhibit alteration features, including corroded margins, dissolution voids and embayments, while others were completely replaced by framboidal pyrite.	The calcite cement appears to have filled macropores before compaction and burial. More coarsely crystalline cemented domains are visible on the core surface (mm scale). These cements are poikilotopic and exhibit non-uniform, orange to bright yellow-orange luminescence when viewed under CL. Minus cement porosity ranges from 15% to 24%. The bright yellow-orange luminescent zones occur towards the centre of larger cement-filled pores, whereas the orange luminescent zones immediately surround detrital quartz grains and fill narrower pore spaces.

Table 1. (Continued).

Palaeosol	Lithology	Pedofeatures	Sphaerosiderites	Cements
Swan River Formation (Yarbo core) 400·85–400·95 m	A silty mudstone with a parallel striated b-fabric (birefringent fabric; Bullock *et al*., 1985) groundmass. The silt is predominantly composed of subangular quartz, with trace amounts of mica and altered feldspar.	This unit exhibits prominent dark orange yellow (10YR 6/6) mottling that is crudely banded parallel to bedding (Fig. 4C). Within the 10YR 6/6 mottled domains are opaque iron oxide and iron sulphide mineral grains. Between the orange-yellow mottles are linear to lens-shaped, very light grey (N7) mottles. This unit generally lacks coatings, with the exception of a few thin (< 30 μm thick), discontinuous and fragmented (highly degraded) clay coatings that show diffuse extinction patterns.	The sphaerosiderites (first described by White *et al*., 2000b) are small (200–350 μm in diameter), and some exhibit spherulitic microstructures with pseudo uniaxial cross-extinction patterns (Fig. 4D). Some nodules show evidence of textural reorganization to blocky mosaic and unit siderite crystals. Some of the nodules underwent fabric-retentive recrystallization as indicated by relict domains of ghost spherulitic microstructure. Many nodules contain minute inclusions of pyrite that occur as aggregates of micron-sized cubes (Fig. 4D). The sphaerosiderites are typically embedded in the orange-yellow mottled domains and often exhibit orange-yellow stains or hypocoatings along the nodule margins.	The very light grey domains are more silt rich and are commonly cemented with poikilotopic calcite. Point counting surveys (300 pts) of the cemented domains indicate that minus cement porosity reaches up to 40% with silt grains floating in an open framework of intergranular porosity filled by calcite cement. The calcite cement displays uniform, bright orange luminescence.
Success S2 Formation, Mannville Group (Shell Mayberries core 16-4-6–5w4) 329·0–329·25 m	A framework-supported muddy sandstone composed of rounded to well-rounded quartz, chert, chalcedony, polycrystalline quartz and rare altered feldspar grains.	This palaeosol lacks any mottling and is generally light grey in colour (N7). Although framework supported, this rock is composed of 30–35% matrix. The matrix is clay dominated and exhibits cross- and granostriated b-fabrics with first-order grey and yellow birefringence. Abundant, thick (100–500 μm), discontinuous and fragmented clay coatings with diffuse to sharp sweeping extinction patterns (moderate to well-ordered clay particles) are present with less common laminated clay and silty-clay infillings that show evidence of degradation (fragmented, deformed laminae). Some of the clay coatings and infillings form compound coatings of clay with superimposed iron oxide hypocoatings.	The sphaerosiderites are very large (2–5 mm diameter) and texturally very complex. The nodules generally consist of four textural domains. First, there are engulfed sand grains coated with 20–40 μm of isopachous siderite cement (Fig. 4E). Secondly, the central portion (core) of the nodule is dominated by dusty, micritic, light brown coloured siderite. Thirdly, a complex system of veins extends through the nodules, and the veins are filled with fine-grained sparry siderite (Fig. 4F). Fourthly, the outer margins of the nodules are constructed of coarse, blocky siderite crystals that are in optical continuity with the vein networks and exhibit sweeping extinction as in spherulites (Fig. 4F). Based upon cross-cutting relationships, the siderite comprising these nodules appears to have been precipitated in the aforementioned sequence.	The matrix contains isolated domains that have been cemented with bright orange luminescent calcite spar, a cement that is generally only visible when viewed under CL (Fig. 3E and F). The calcite-cemented domains are very small (a few 100 μm in diameter) irregular patches, most often observed directly adjacent to sphaerosiderite nodules.

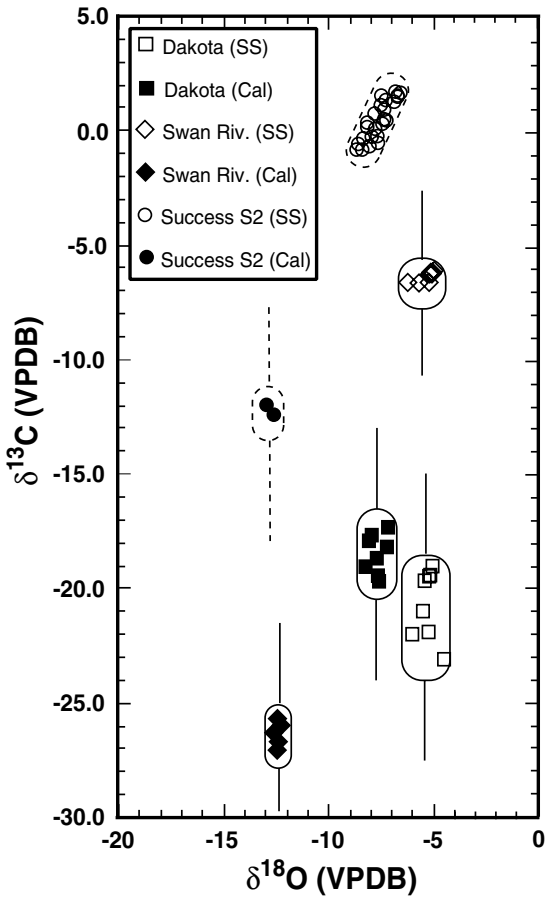

Fig. 6. Compiled $\delta^{18}O$ vs. $\delta^{13}C$ values of sphaerosiderites and calcite cements from the Dakota, Swan River and Success S2 Formations. The vertical lines indicate MSL (the average siderite $\delta^{18}O$ value) and MCL (average calcite $\delta^{18}O$ value) oxygen isotopic values, and the ovals envelop the range of values for that particular palaeosol.

palaeolatitudes for each given study area (Fig. 10). The Dakota Formation in the Jones #1 core in Kansas was deposited at 34°N palaeolatitude, and the mean annual temperature was ≈27 °C (ranged from 23 °C to 32 °C) (Barron, 1983). Groundwater $\delta^{18}O_{VSMOW}$ values calculated from the sphaerosiderites were determined to range between −7·10‰ and −5·03‰, and those for the calcite cement were between −6·26‰ and −4·42‰. The Swan River Formation (45°N palaeolatitude, mean annual temperature 25 °C, range 19–29 °C) yields groundwater $\delta^{18}O_{VSMOW}$ values ranging from −8·00‰ to −5·62‰ from sphaerosiderites and from −11·73‰ to −9·63‰ from the calcite cements. The Success S2 Formation (46°N, mean annual temperature 24·7 °C, range 19–28 °C) yields groundwater $\delta^{18}O_{VSMOW}$ values ranging from −10·39‰ to −8·23‰ from the sphaerosiderites and from −12·16‰ to −10·26‰ from the calcite cements.

DISCUSSION

Preservation of early diagenetic sphaerosiderite compositions

One of the primary goals of this investigation was to determine the extent to which original, early diagenetic sphaerosiderite isotopic values might be recovered from palaeosol units significantly overprinted by later diagenesis.

Dakota Formation

Sphaerosiderites in the 87·8 m depth interval of the KGS Jones core exhibit significant internal textural reorganization (Fig. 5A and B). Microprobe transects across several nodules showed that the cores of the texturally altered sphaerosiderites are consistently comprised of > 88 mol% $FeCO_3$ and have highly variable Mg/Fe and Mg/(Ca+Mg) ratios. This suggests changing porewater compositions during precipitation, rate-induced differences in the distribution coefficients or perhaps significant elemental substitutions during recrystallization. Milling of nodule centres, however, yielded isotopic values that define an MSL (−5·3‰ VPDB) with a relatively low $\delta^{18}O$ standard deviation (0·43‰).

The MSL from the 87·8 m sample has $\delta^{18}O$ values comparable with other sphaerosiderite-bearing horizons from the Dakota Formation in the KGS Jones core (MSLs of −5·1‰ and −5·8‰ VPDB). Apparently, recrystallization did not significantly affect the $^{18}O/^{16}O$ ratios in the core of the siderite nodules. Thus, despite the textural and compositional alterations, the sphaerosiderites of this unit do retain a geochemical 'memory' of early diagenesis.

Swan River Formation

In a previous study (White *et al.*, 2000b), linear covariant $\delta^{18}O$ vs. $\delta^{13}C$ trends were reported from sphaerosiderites of the SGS Yarbo core. White *et al.* (2000b) posited several hypotheses to explain the covariant isotopic trends ($\delta^{18}O_{VPDB}$ values ranging between −9·25‰ and −3·75‰), including later diagenetic overprinting. Based on the initial conclusions of White *et al.* (2000b), these samples were subjected to closer petrographic scrutiny to assess the importance of diagenetic overprinting. Additional microsampling along with acetic acid leaching to ensure

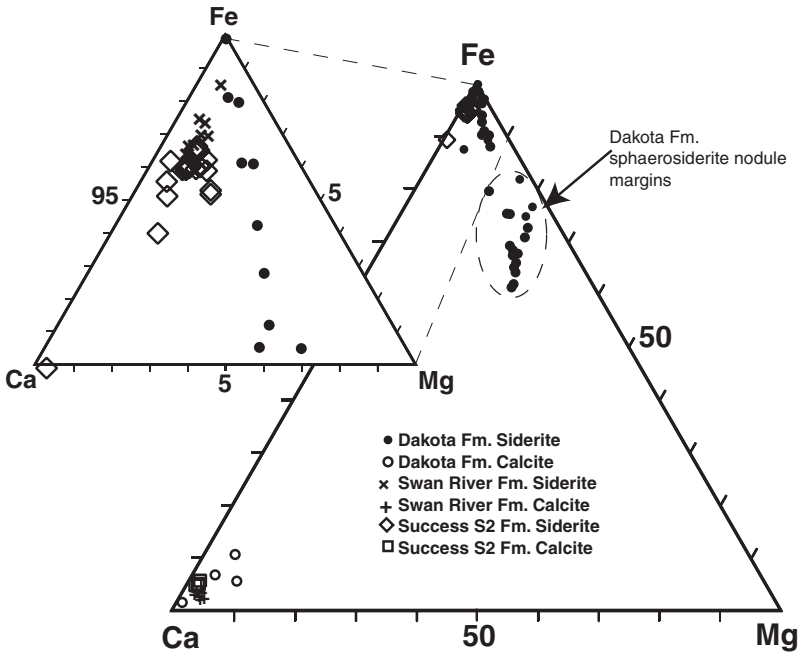

Fig. 7. Composite ternary diagram showing the relative Fe, Ca and Mg compositions of the Dakota, Swan River and Success S2 Formation sphaerosiderites and calcite cements (electron microprobe data). The dashed oval field envelopes compositions determined for the margins of siderite nodules in the Dakota Formation sample.

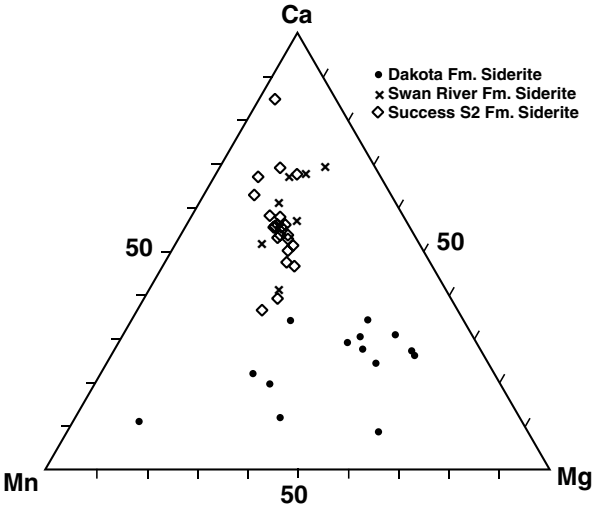

Fig. 8. Composite ternary diagram showing the relative Ca, Mn and Mg compositions of the Dakota, Swan River and Success S2 Formation siderites (electron microprobe data). The Dakota Formation compositions represent analyses of siderite nodule cores only.

isolation of siderite did not reproduce the linear covariant trends reported by White *et al.* (2000b); however; the new data support the contention that early diagenetic signals are preserved. New analyses from both the 400·85 m and the 400·95 m depth intervals produced a cluster of points ($\delta^{18}O_{VPDB}$ values ranging from −6·26‰ to −5·00‰) with a $\delta^{18}O$ standard deviation of 0·38‰. The low standard deviation in $\delta^{18}O$ compositions implies precipitation from a stable groundwater system (Ludvigson *et al.*, 1998). Recovery of an

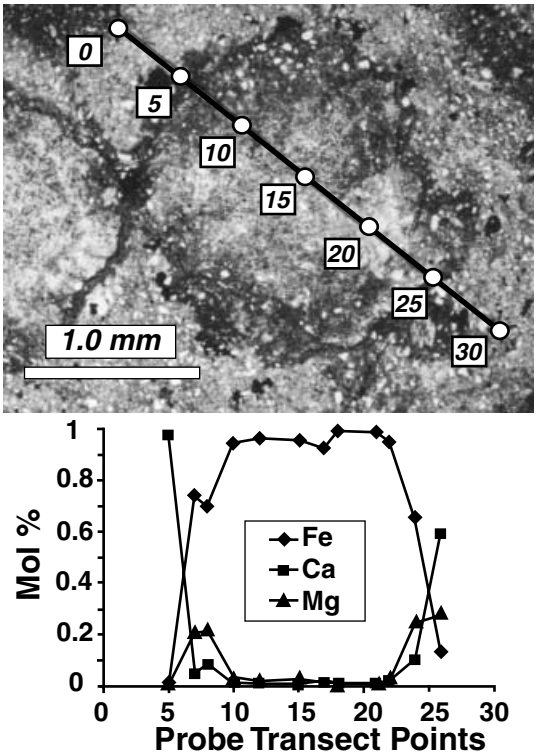

Fig. 9. Photomicrograph of a siderite nodule in the Dakota Formation 87·8–87·9 m sample illustrating a linear microprobe transect taken across the nodule and the adjacent matrix. Note how the mol% of Fe decreases from the core of the nodule outwards into the groundmass, and Ca and Mg increase in the nodule margins and groundmass.

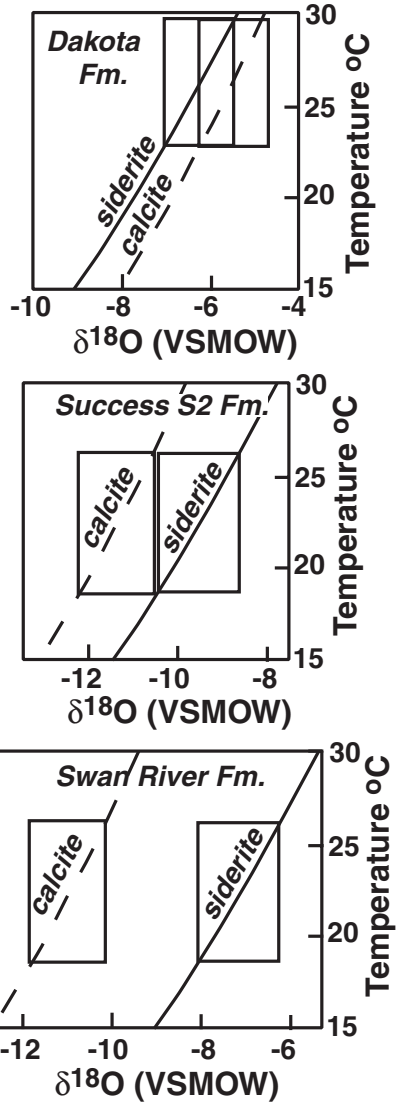

Fig. 10. Mid-Cretaceous groundwater compositions calculated from sample MSL and MCL values over a range of temperatures (0–30 °C). The rectangles define a range of mean annual temperatures for the site determined from a 4 × CO_2 atmosphere palaeoclimate model simulation (acquired from Barron *et al.*, 1995).

early diagenetic signal is further substantiated by the MC-57 sphaerosiderite compositions first reported by Ludvigson *et al.* (1998) from an outcrop of the Swan River Formation in western Manitoba. These data produce invariant $\delta^{18}O$ values (MSL = −5·5‰ VPDB) that are nearly identical in composition to the SGS Yarbo core samples analysed in this study (see Fig. 3 of White *et al.*, 2000b).

The minor element analyses of the Yarbo core sphaerosiderites also support the concept of preservation of early diagenetic $\delta^{18}O$ and $\delta^{13}C$ compositions. The nodules are fairly pure $FeCO_3$ and exhibit only minor substitutions of Ca, Mg and Mn (Figs 7 and 8). Furthermore, the Mg/Fe and Mg/(Ca+Mg) ratios are very low, suggesting precipitation from purely meteoric groundwater (Matsumoto & Iijima, 1981; Mozley, 1989; Brown & Kingston, 1993).

Success S2 Formation

Evaluating the preservation of early diagenetic isotopic compositions in the sphaerosiderites of the Success S2 Formation is more difficult. The covariant isotopic trends are interpreted as resulting from compositional variations in the nodule textural components; however, the isopachous siderite grain coatings and siderite-filled veins are too small scale for current sampling procedures. The minor element data suggest that some of the veins and siderite nodule margins have increased substitutions of Mg^{2+} and Ca^{2+} however, there is no distinct difference in the elemental composition of the various components. Analyses of homogenized microsamples from the nodule cores and margins were compared, and no statistically significant differences were noted. The depleted end-member compositions probably reflect early meteoric compositions (Ludvigson *et al.*, 1996); however, fluid mixing calculations (described below) provide a better assessment of the compositional trends.

Fluid mixing model. Fluid mixing mass balance calculations assuming closed system conditions were used to generate hyberbolic mixing trends depicting a range of possible siderite compositions forming under mixtures of fluids of differing $\delta^{18}O$, $\delta^{13}C$ and ΣCO_2. Two hyperbolic mixing curves were generated to constrain the Success S2 sphaerosiderite covariant $\delta^{18}O$ vs. $\delta^{13}C$ trend. The water compositions range between two end-members. The enriched end-member (modified sea water) was modelled with the following input values: a $\delta^{18}O_{VSMOW}$ value of −1‰, $\delta^{13}C_{VPDB}$ value of +3·0‰, and the total dissolved carbon (ΣCO_2) composition was estimated to be 2·5 mmol l^{-1}. The isotopic distinction between an open-marine and modified marine phreatic fluid relates to the $\delta^{13}C$ compositions that are enriched relative to the PDB standard (Ludvigson *et al.*, 1994). The depleted end-member (meteoric groundwater) was modelled with a $\delta^{18}O_{VSMOW}$ value of −9·50‰ and $\delta^{13}C_{VPDB}$ values ranging between −5·00‰ and −3·00‰ with ΣCO_2 values ranging between 1·75 and 0·75 mmol l^{-1} respectively. The resulting (model output) siderite $\delta^{18}O$ and $\delta^{13}C$ compositions that would be precipitated

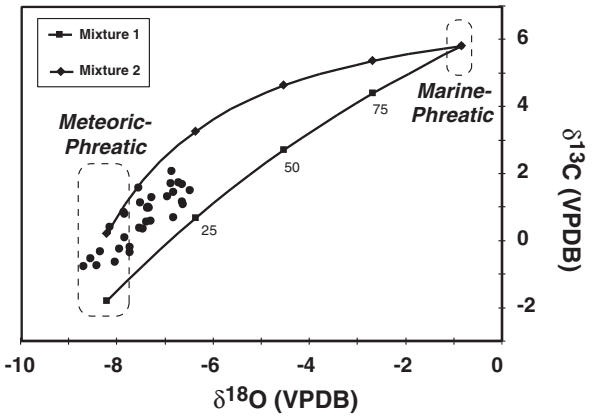

Fig. 11. The hyperbolae represent possible siderite isotopic values ranging between meteoric and marine end-member values based upon mixing variable amounts of marine phreatic and meteoric phreatic waters. The curves were modelled to envelop the range of empirical sphaerosiderite values. The squares and diamonds represent 25%, 50% and 75% mixtures (i.e. the 25 indicates 25% marine phreatic, 75% meteoric phreatic), and thus show that the Success S2 Formation compositions were influenced by less than 25% marine phreatic fluid mixing with the meteoric phreatic groundwater.

from variable mixtures of these fluids are illustrated in Fig. 11 (mixtures 1 and 2). The siderite $\delta^{18}O_{VPDB}$ values range between −0·84‰ and −8·20‰, and the $\delta^{13}C_{VPDB}$ compositions range between +5·80‰ and −1·81‰ (mix 1) and +0·20‰ (mix 2).

Later diagenesis

Swan River Formation

The 400·85–400·95 m palaeosol of the Swan River Formation exhibits two phases of carbonate precipitation. The first phase is represented by sphaerosiderite precipitation in a shallow, reducing, meteoric groundwater system. Calcite precipitation and occlusion of intergranular porosity in the coarser grained domains of the palaeosol characterize the second and later phase. The $\delta^{18}O$ values of the early diagenetic sphaerosiderites reflect the isotopic compositions of the soil groundwater systems in a small catchment area recharged by coastal precipitation (Ludvigson *et al.*, 1998). Lithofacies analyses show that the palaeosols were closely associated with estuarine and marine deposits, indicating that they formed in lower coastal plain palaeoenvironments (Ludvigson *et al.*, 1996, 1998). The later calcite cements precipitated in a groundwater flow system, the fluids of which had more depleted $\delta^{18}O$ values as a consequence of recharge by upstream catchment basin drainage, and reflect the homogenized isotopic composition of much larger catchment areas in which palaeoprecipitation was influenced by 'continental effects' (Dansgaard, 1964; Rozanski *et al.*, 1993). Trends of decreasing precipitation $\delta^{18}O$ values extending inland away from the coast, which result from air masses migrating over a continent, losing moisture through precipitation and preferentially removing the heavier H_2O molecules (contain ^{18}O atoms) with distance from the coast, are what Dansgaard (1964) referred to as 'continental effects'. Contours of precipitation–evaporation from models of the Turonian suggest that significant amounts of precipitation extended (west to east) across the cratonic landmass of North America, which drained back into the Western Interior Seaway through long, east–west-trending drainage basins at a rate of $\approx 2{\cdot}6 \times 10^{12}$ m^3 year^{-1} (Slingerland *et al.*, 1996).

The $\delta^{18}O$ values of the calcite cements indicate that shallow groundwaters have been recharged by isotopically light inland palaeoprecipitation, that the $\delta^{18}O$ values have not been significantly changed through rock–water interactions and that precipitation of the calcite occurred at shallow burial depths (insignificant geothermal gradients). Shallow burial depths are indicated by high intergranular volumes (up to 40%) and lack of quartz grain point contacts, recording cementation before the collapse of intergranular porosity through burial compaction (Maxwell, 1964; Houseknecht, 1984, 1987). Substantial variations in fluid ^{18}O compositions resulting from rock–water interaction in the regional flow system are not indicated, as the isotopic trends of meteoric calcite lines seen in these cements show that fluid $\delta^{18}O$ was not a major variable. Extensive rock–water interaction should generally lead to more variable $\delta^{18}O$ relative to the $\delta^{13}C$ variations that approach host rock (aquifer) compositions (Carpenter *et al.*, 1988; Lohmann, 1988); however, oxygen isotope exchange in the shallow groundwaters of a host rock dominated by stable silicate minerals is unlikely.

Success S2 Formation

The isotopic compositions obtained from the sphaerosiderites of the Success S2 Formation exhibit a distinctive positive covariant $\delta^{18}O$ vs. $\delta^{13}C$ compositional trend that is somewhat reminiscent of the 'inverted J curve' of Meyers & Lohmann (1985) and Lohmann (1988; Figs 6 and 11). Such a trend may develop through siderite precipitation from fluids that evolved

compositionally over time or from mixing of compositionally distinct fluids (Carpenter *et al.*, 1988; Lohmann, 1988). Evolution of the diagenetic fluid composition through sediment–water interaction (large volumes of dissolved siderite cycled through precipitation–dissolution reactions in a small volume of fluid) is highly unlikely in this diagenetic system considering that sphaerosiderites develop in wetland soil environments (Stoops, 1983; Landuydt, 1990) with high water/rock ratios. A more plausible explanation for this isotopic compositional trend is sphaerosiderite precipitation from a mixture of two different diagenetic fluids (Ludvigson *et al.*, 1996). The resulting water compositions range between modified marine phreatic (enriched $\delta^{18}O$ and $\delta^{13}C$ values) and meteoric phreatic (depleted) end-member compositions (Ludvigson *et al.*, 1996). Mixing of marine and meteoric fluids during the precipitation of these nodules is further supported by the electron microprobe data indicating some compositional variations between the various textural components. The decreased mol% $FeCO_3$ and increased Ca content of the fine veins and nodule margins support the influence of marine-derived fluids upon siderite precipitation (Matsumoto & Iijima, 1981; Mozley, 1989). These substitutions are also reflected in the variable Mg/Fe and Mg/(Ca+Mg) ratios, where the highest ratios are from the veins and nodule margins. Based upon the modelled hyperbolic trends, the diagenetic fluids never exceeded 20–25% modified marine fluid.

The calcite cements represent a later phase of carbonate precipitation. Similar to the Swan River Formation sample, these cements are also interpreted to have precipitated from meteoric fluids that integrated regional recharge from upstream catchment basin drainage (Fig. 12).

Dakota Formation

A three-stage diagenetic history is recorded in the KGS Jones #1 core 87·8–87·9 m depth interval. First, sphaerosiderite precipitation occurred in a local soil water meteoric–phreatic groundwater flow system. Secondly, infiltration of modified marine phreatic fluids (during local sea-level rise) penetrated the palaeosol complex inducing sphaerosiderite replacement by pyrite and siderite recrystallization. Thirdly, extensive precipitation of poikilotopic calcite cement occurred in a different meteoric phreatic fluid with a slightly different composition (Fig. 13).

The abundance of pyrite in this sample suggests that marine fluids influenced shallow burial diagenesis of the palaeosol (Carpenter *et al.*, 1988; Fig. 5B). Pyrite indicates an abundance of dissolved sulphate and reactive organic matter for the production of H_2S (Berner, 1981; Carpenter *et al.*, 1988; Pye *et al.*, 1990). The S_2 hydrocarbons and the total organic carbon (TOC) content of the sample, as determined by Rock-Eval pyrolysis (Young, 2002), also indicate marine influence. The 87·8–87·9 m sample plots in the type II kerogen field on a TOC vs. S2 diagram, suggesting that the organic matter had a marine origin (Espitalié *et al.*, 1985; Langford & Blanc-Valleron, 1990; Fig. 14). The deposits directly overlying the 87·8 m horizon (87·5–85·7 m interval, Fig. 2) have type I kerogen compositions, suggesting that the

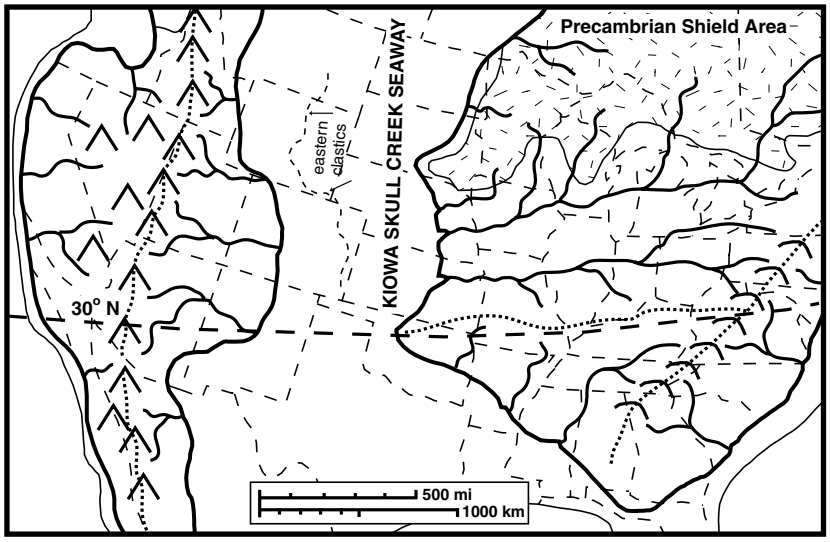

Fig. 12. Mid-Cretaceous palaeogeographic reconstruction of N. America depicting hypothetical river drainage systems. The fine dashed lines indicate major drainage divides. The coarse subcontinent outlines depict palaeoshoreline positions during maximum transgression of the Kiowa–Skull Creek Seaway during the Late Albian. The maximum westward extent of eastern-sourced siliciclastics is also shown (arrows pointing to dashed line; modified from Witzke & Ludvigson, 1996).

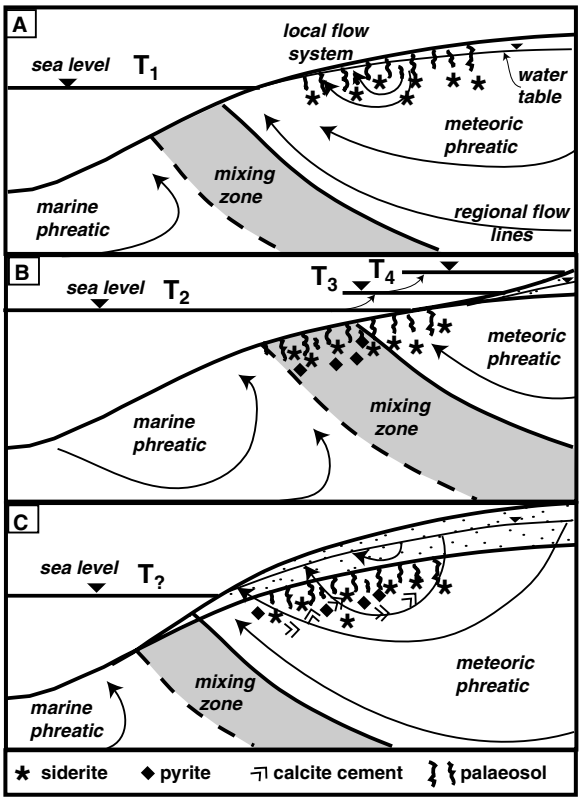

Fig. 13. Cartoon illustrating the three-stage diagenetic history recorded in the 87·8 m sample of the KGS Jones #1 core. (A) First, sphaerosiderites were forming in coastal plain alluvium close to sea level (T1 = time 1) in a local, shallow, groundwater flow system that was recharged by palaeoprecipitation. (B) Secondly, under conditions of rising sea level (T2, T3 and T4…), the paleosols were inundated by modified marine phreatic fluids, possibly in the mixing zone between the meteoric and marine phreatic zones, and sphaerosiderite alteration, and replacement by pyrite occurred. (C) Thirdly, later ($T_?$), under conditions of lowered sea level, cross-formational flow of later meteoric phreatic fluids down through the buried palaeosols precipitated the calcite cement.

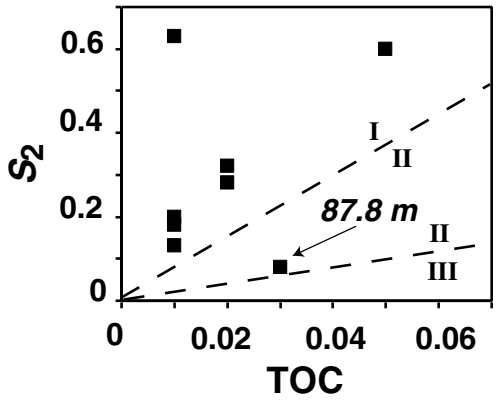

Fig. 14. An S_2 vs. TOC diagram of samples collected at 1-foot intervals from the KGS Jones #1 core between 281 feet (85·7 m) and 288 feet (87·8 m) (Young, 2002). The 87·8 m sample is labelled, and it plots in the type II kerogen field, suggesting that the organic matter had a marine origin. The overlying samples all fall within the type I kerogen field, suggesting that the organic matter had a lacustrine origin. S_2 is in milligrams of hydrocarbon per gram of rock (mg HC/g rock), and TOC is the number of grams of TOC per 100 g of rock.

organic matter was lacustrine (Langford & Blanc-Valleron, 1990; Fig. 14).

The cation compositional trends in the recrystallized sphaerosiderites suggest precipitation from modified marine phreatic fluids. The cores are relatively pure siderite (> 95 mol% $FeCO_3$), and the margins show significant enrichments in Mg^{2+} and Ca^{2+}. Siderite precipitated in freshwater environments is typically very pure, containing >90 mol% $FeCO_3$ (Mozley, 1989). Marine waters have higher Mg^{2+} and Ca^{2+} concentrations and greater Mg^{2+}/Ca^{2+} ratios than meteoric waters (Carpenter *et al.*, 1988; Mozley, 1989). The sphaerosiderites also exhibit increased Mg/(Ca+Mg) ratios towards the margins of the nodules. Matsumoto & Iijima (1981) suggested that increased Mg/(Ca+Mg) ratios in siderite concretions from Palaeogene coal measures in Japan resulted from precipitation in freshwaters that mixed with Mg-rich brines that dewatered from interbedded (compacting) marine deposits.

Dissolution of the sphaerosiderites and precipitation of the pyrite are interpreted to have been coeval processes in a diagenetic system with mixed marine meteoric phreatic fluids. Pyrite precipitated after siderite because iron carbonates cannot form in the sulphate reduction zone in the presence of dissolved sulphide (Hesse, 1990). Precipitation of pyrite scavenged Fe^{2+} from dissolving sphaerosiderites and decreased the Fe^{2+}/Mg^{2+} and Fe^{2+}/Ca^{2+} ratios in the ambient fluid (Curtis & Coleman, 1986; Mozley & Carothers, 1992). Exhaustion of dissolved sulphide as sulphate-reducing bacteria consumed available dissolved sulphate probably terminated pyrite precipitation. However, the increased Mg^{2+} and Ca^{2+} concentrations in the fluid led to increased cation substitutions during subsequent recrystallization of the remaining siderite nodules particularly around nodule margins.

The low $\delta^{18}O$ values (−8·3‰ to −7·3‰ VPDB) and $\delta^{13}C$ values (−21·7‰ to −17·3‰ VPDB) of the calcite cement indicate precipitation from meteoric fluids (Allan & Matthews, 1977, 1982; Meyers & Lohmann, 1985; Carpenter *et al.*, 1988; Lohmann, 1988). The texture of the poikilotopic calcite spars argues for calcite precipitation in a

meteoric phreatic setting (Folk, 1974). The calcite-filled macropores probably produced a rigid framework about which other soil components were deformed during burial compaction. Thermal maturation analyses suggest that these cements formed at shallow depths, as the Cretaceous of central Kansas attained a maximum burial depth of 460 m, and burial temperatures were no more than 25 °C greater than the surface temperatures (Newell, 1997). If the calcite cements had precipitated coeval with the pyrite, the isotopic compositions of the calcite would probably define a covariant $\delta^{18}O$ vs. $\delta^{13}C$ trend approaching marine end-member compositions (i.e. enriched $\delta^{13}C$ and $\delta^{18}O$ values).

The textural and geochemical data suggest that diagenesis in this palaeosol was closely linked to changes in relative sea level. Aggradation of coastal plain deposits associated with transgression of the Western Interior Seaway buried the palaeosols. Then, fluid advection, possibly related to tidal pumping, mixed marine waters with the meteoric phreatic groundwater lens (Ludvigson *et al.*, 1996). Mixing of the marine and meteoric fluids produced a diagenetically aggressive fluid that altered the sphaerosiderites as described previously. Subsequent progradation and/or eustatic sea-level fall and retreat of marine phreatic fluids re-established a fully meteoric phreatic system from which the calcite cements precipitated. The fact that the calculated groundwater compositions from a calcite cement defining an MCL (Lohmann, 1988) are enriched by +0·7‰ relative to the precipitating fluid for the sphaerosiderites suggests that the calcite cements also formed in a groundwater flow system recharged by local coastal precipitation.

CONCLUSIONS

1 The sphaerosiderites examined in this study have all sustained variable degrees of alteration in the presence of later, diagenetically aggressive fluids resulting in both textural and compositional changes. Despite these changes, the siderites have retained the original $\delta^{18}O$ values reflecting the isotopic composition of the soil water (meteoric fluids) from which they precipitated. However, recovering the early diagenetic $\delta^{18}O$ and $\delta^{13}C$ values involved the examination of all carbonate phases present, including isotopic and minor element compositional trends within individual nodules.

2 The Swan River Formation palaeosols contain sphaerosiderites (a proxy for 'local', coastal meteoric compositions) and poikilotopic calcite cements (a proxy for 'regional', meteoric phreatic compositions in a cratonic palaeoaquifer system). The sphaerosiderites formed in shallow groundwater flow systems with small catchment areas recharged by coastal precipitation. The calcite cements precipitated from regional groundwater flow systems that integrated inland palaeoprecipitation from much larger catchment areas.

3 Covariant, hyperbolic trends in the $\delta^{18}O$ vs. $\delta^{13}C$ compositions of sphaerosiderites may result from precipitation from groundwater systems resulting from mixing of modified marine and meteoric phreatic fluids. The sphaerosiderites in the Success S2 Formation example are texturally complex, and the isotopic compositions yield a covariant, hyperbolic trend that suggests mixing of up to 15–25% marine fluids with meteoric fluids in the groundwater flow system. The elevated Ca^{2+} and Mg^{2+} concentrations in the veined and exterior domains of the siderite nodules further supports mixing of marine and meteoric fluids. The light end-member $\delta^{18}O$ values of these nodules reflect purely meteoric fluid compositions, whereas the heavy end-members reflect mixed (meteoric marine) fluid compositions.

ACKNOWLEDGEMENTS

This project was supported by NSF grant #EAR 96-28128 and by the University of Iowa Center for Global and Regional Environmental Research. A Geological Society of America research grant and Department of Education GAANN grant supported the senior author. Thanks to T. White, K. Saville, L. Young and P. L. Phillips for assistance with sample collection and preparation, and S. J. Carpenter, L. Wingate and K. C. Lohmann for isotopic analyses. Leah Young and Dr Tim White obtained the Rock-Eval pyrolysis data from the KGS Jones #1 core, and Dr John Doveton of the Kansas Geological Survey was very helpful in arranging funding support for this work. Special thanks to Dr Dale Leckie for providing the Success S2 Formation samples and core descriptions. Thanks also to Dr Peter McSwiggen, director of the University of Minnesota Electron Microprobe Laboratory. We thank Dr James Boles and Dr Peter Mozley for their thorough and thoughtful reviews of this manuscript.

REFERENCES

Allan, J.R. and **Matthews, R.K.** (1977) Carbon and oxygen isotopes as diagenetic and stratigraphic tools: data from surface and subsurface of Barbados, West Indies. *Geology*, **5,** 16–20.

Allan, J.R. and **Matthews, R.K.** (1982) Isotope signatures associated with early meteoric diagenesis. *Sedimentology*, **29,** 797–818.

Barron, E.J. (1983) A warm and equable Cretaceous: the nature of the problem. *Earth-Sci. Rev.*, **19,** 305–338.

Barron, E.J., Fawcett, P.J., Peterson, W.H., Pollard, D. and **Thompson, S.L.** (1995) A 'simulation' of mid-Cretaceous climate. *Paleoceanography*, **10,** 953–962.

Berner, R.A. (1981) A new classification of sedimentary environments. *J. Sed. Petrol.*, **51,** 359–365.

Brenner, R.L., Ludvigson, G.A., Witzke, B.J., Zawistoski, A.N., Kvale, E.P., Ravn, R.L. and **Joeckel, R.M.** (2000) Late Albian Kiowa-Skull Creek Marine Transgression, Lower Dakota Formation, Eastern Margin of Western Interior Seaway, USA. *J. Sed. Res.*, **70,** 868–878.

Brown, G.H. and **Kingston, D.M.** (1993) Early diagenetic spherulitic siderites from Pennsylvanian paleosols in the Boss Point Formation, Maritime Canada. *Sedimentology*, **40,** 467–474.

Bullock, P., Fedoroff, N., Jongerius, A., Stoops, G., Tursina, T. and **Babel, U.** (1985) *Handbook for Soil Thin Section Description*, 152 pp. Waine Research Publications, Wolverhampton.

Carothers, W.W., Lanford, H.A. and **Rosenbauer, R.J.** (1988) Experimental oxygen isotope fractionation between siderite-water and phosphoric acid liberated CO_2-siderite. *Geochim. Cosmochim. Acta*, **52,** 2445–2450.

Carpenter, S.J., Erickson, M.J., Lohmann, K.C. and **Owen, M.R.** (1988) Diagenesis of fossiliferous concretions from the Upper Cretaceous Fox Hills Formation, North Dakota. *J. Sed. Petrol.*, **52,** 792–814.

Curtis, C.D. and **Coleman, M.L.** (1986) Controls on the precipitation of early diagenetic calcite, dolomite, and siderite concretions in complex depositional sequences. In: *Roles of Organic Matter in Sediment Diagenesis* (Ed. D.L. Gautier), *SEPM Spec. Publ.*, **38,** 23–33.

Dansgaard, W. (1964) Stable isotopes in precipitation. *Tellus*, **16,** 436–468.

Espitalié, J., Deroo, G. and **Marquis, F.** (1985) La pyrolyse Rock-Eval et ses applications. *Rev. Inst. Fr. Pétrol.*, **40,** 563–579 & 755–784.

Folk, R.L. (1974) *Petrology of Sedimentary Rocks*. Hemphill Publishing, Austin, TX, 182 pp.

Friedman, I. and **O'Neil, J.R.** (1977) Compilation of stable isotope fractionation factors of geochemical interest. *US. Geol. Surv. Prof. Paper*, **P0440-KK,** 12 pp.

Hamilton, V. (1994) Sequence stratigraphy of Cretaceous Albian and Cenomanian strata in Kansas. In: *Perspectives on the Eastern Margin of the Cretaceous Western Interior Basin* (Eds G.W. Shurr, G.A. Ludvigson and R.H. Hammond), *Geol. Soc. Am. Spec. Paper*, **287,** 79–96.

Hesse, R. (1990) Early diagenetic pore water/sediment interaction. In: *Diagenesis* (Eds I.A. Mcllreath and D.W. Morrow), Geoscience Canada Reprints Series 4, pp. 277–316. Geological Association of Canada, Department of Earth Sciences, Memorial University of Newfoundland, St John's, Canada.

Houseknecht, D.W. (1984) Influence of grain size and temperature on intergranular pressure solution, quartz cementation, and porosity in a quartzose sandstone. *J. Sed. Petrol.*, **54,** 348–361.

Houseknecht, D.W. (1987) Assessing the relative importance of compaction processes and cementation to reduction of porosity in sandstones. *AAPG Bull.*, **71,** 633–642.

Joeckel, R.M. (1987) Paleogeomorphic significance of two paleosols in the Dakota Formation (Cretaceous), southeastern Nebraska. *Univ. Wyoming Contrib. Geol.*, **25,** 95–102.

Landuydt, C.J. (1990) Micromorphology of iron minerals from bog ores of the Belgian Campine area. In: *Soil Micromorphology. A Basic and Applied Science* (Ed. L.A. Douglas), , Developments in Soil Science **19,** pp. 289–294. Elsevier, Amsterdam.

Langford, F.F. and **Blanc-Valleron, M.-M.** (1990) Interpreting Rock-Eval pyrolysis data using graphs of pyrolizable hydrocarbons vs. total organic carbon. *AAPG Bull.*, **74,** 799–804.

Leckie, D., Vanbeselaere, N.A. and **James, D.P.** (1995) Regional stratigraphic picks for the Mannville Group – southwestern Saskatchewan, Phase 1. *Geol. Surv. Can. Open File Rep.*, **3109,** 10 pp.

Leckie, D.A., Vanbeselaere, N.A. and **James, D.P.** (1997) Regional sedimentology, sequence stratigraphy and petroleum geology of the Mannville Group: southwestern Saskatchewan. In: *Petroleum Geology of the Cretaceous Mannville Group, Western Canada* (Eds S.G. Pemberton and D.P. James), *Can. Soc. Petrol. Geol. Mem.*, **18,** 211–262.

Lohmann, K.C. (1988) Geochemical patterns of meteoric diagenetic systems and their application to studies of paleokarst. In: *Paleokarst* (Eds N.P. James and P.W. Choquette), pp. 58–80. Springer Verlag, New York.

Ludvigson, G.A., Witzke, B.J., González, L.A., Hammond, R.H. and **Plocher, O.W.** (1994) Sedimentology and carbonate geochemistry of concretions from the Greenhorn marine cycle (Cenomanian-Turonian), eastern margin of the Western Interior Seaway. In: *Perspectives on the Eastern Margin of the Cretaceous Western Interior Basin* (Eds G.W. Shurr, G.A. Ludvigson and R.H. Hammond), *Geol. Soc. Am. Spec. Paper*, **287,** 145–173.

Ludvigson, G.A., González, L.A., Witzke, B.J., Brenner, R.L. and **Metzger, R.A.** (1996) Diagenesis of iron minerals in the Dakota Formation. In: *Mid-Cretaceous Fluvial Deposits of the Eastern Margin, Western Interior Basin: Nishnabotna Member, Dakota Formation. A Field Guide to the Cretaceous of Guthrie County, North Central GSA Annual Meeting, Ames, Iowa, Field Trip No. 1* (Eds B.J. Witzke and G.A. Ludvigson), *Iowa Geol. Surv. Bur. Guidebook Series*, **17,** 31–38.

Ludvigson, G.A., González, L.A., Metzger, R.A., Witzke, B.J., Brenner, R.L., Murillo, A.P. and **White, T.S.** (1998) Meteoric sphaerosiderite lines and their use for paleohydrology and paleoclimatology. *Geology*, **26,** 1039–1042.

Ludvigson, G.A., Ufnar, D.F., González, L.A., White, T.S., Phillips, P.L., Witzke, B.J. and **Brenner, R.L.** (2000) When good sphaerosiderites go bad: caveats in the application of a paleoclimate proxy. *Geol. Soc. Am. Abstract with Progs*, A-524.

Macfarlane, P.A. and **Hamilton, V.J.** (1990) The impact of the aquifer framework on groundwater flow in the Dakota aquifer of Kansas. *AAPG Bull.*, **74,** 710–711.

Macfarlane, P.A., Doveton, J.H., Feldman, H.R., Butler, J.J., Jr and **Combes, J.M.** (1994) Aquifer/aquitard units of the Dakota aquifer system in Kansas; methods of delineation and sedimentary architecture effects on ground-water flow and flow properties. *J. Sed. Res.*, **64,** 464–480.

McNeil, D.H. and **Caldwell, W.G.E.** (1981) Cretaceous rocks and their foraminifera in the Manitoba Escarpment. *Geol. Assoc. Can. Spec. Paper*, **21,** 439 pp.

Matsumoto, R. and **Iijima, A.** (1981) Origin and diagenetic evolution of Ca-Mg-Fe carbonates in some coalfields of Japan. *Sedimentology*, **28,** 239–259.

Maxwell, J.C. (1964) Influence of depth, temperature, and geologic age on porosity of quartzose sandstone. *AAPG Bull.*, **48,** 697–709.

Meyers, W.J. and **Lohmann, K.C.** (1985) Isotope geochemistry of regionally extensive calcite cement zones and marine components in Mississippian limestones, New Mexico. In: *Carbonate Cements* (Eds N. Schneidermann and P.M. Harris), *SEPM Spec. Paper*, **36,** 223–239.

Mozley, P.S. (1989) Relation between depositional environment and the elemental composition of early diagenetic siderite. *Geology*, **17,** 704–706.

Mozley, P.S. and **Carothers, W.W.** (1992) Elemental and Isotopic composition of siderite in the Kuparuk Formation, Alaska. effect of microbial activity and water/sediment interaction on early pore-water chemistry. *J. Sed. Res.*, **62,** 681–692.

Newell, K.D. (1997) Comparison of maturation data and fluid-inclusion homogenization temperatures to simple thermal models; implications for thermal history and fluid flow in the midcontinent. In: *Current Research in Earth Sciences* (Ed. L. Brosius), *Kansas Geol. Surv. Bull*, **240,** 13–27.

Playford, G. (1971) Palynology of Lower Cretaceous (Swan River) strata of Saskatchewan and Manitoba. *Paleontology*, **14,** 533–565.

Price, L.L. (1963) Lower Cretaceous rocks of southeastern Saskatchewan. *Geol. Surv. Can. Paper*, **62-29,** 55 pp.

Pye, K., Dickson, J.A.D., Schiavon, N., Coleman, M.L. and **Cox, M.** (1990) Formation of siderite-Mg-calcite-iron sulphide concretions in intertidal marsh and sandflat sediments, north Norfolk, England. *Sedimentology*, **37,** 325–343.

Rozanski, K., Araguas-Araguas, L. and **Gonfiantini, R.** (1993) Isotopic patterns in modern global precipitation. In: *Climate Change in Continental Isotopic Records* (Eds B.K. Swart, K.C. Lohman, J. McKenzie and S. Savin), *Am. Geophys. Union Geophys. Monogr.*, **78,** 1–36.

Scotese, C.R. (1991) Jurassic and Cretaceous plate tectonic reconstructions. *Palaeogeogr. Palaeoclimatol. Palaeoecol.*, **87,** 493–501.

Slingerland, R., Kump, L.R., Arthur, M.A., Fawcett, P.J., Sageman, B.B. and **Barron, E.J.** (1996) Estuarine circulation in the Turonian Western Interior seaway of North America. *Geol. Soc. Am. Bull.*, **108,** 941–952.

Spicer, R.A. and **Corfield, R.M.** (1992) A review of terrestrial and marine climates in the Cretaceous with implications for modeling the 'Greenhouse Earth'. *Geol. Mag.*, **129,** 169–180.

Stoops, G. (1983) SEM and light microscopic observations of minerals in bog-ores of Belgian Campine. *Geoderma*, **30,** 179–186.

Ufnar, D.F., González, L.A., Ludvigson, G.A., Brenner, R.L. and **Witzke, B.J.** (2001) Stratigraphic implications of meteoric sphaerosiderite $\delta^{18}O$ compositions in paleosols of the Cretaceous (Albian) Boulder Creek Formation, NE British Columbia Foothills, Canada. *J. Sed. Res.*, **71,** 1017–1028.

Ufnar, D.F., González, L.A., Ludvigson, G.A., Brenner, R.L. and **Witzke, B.J.** (2002) The mid-Cretaceous water bearer: isotope mass balance quantification of the Albian hydrologic cycle. *Palaeogeogr. Palaeoclimatol. Palaeoecol.*, **188,** 51–71.

White, T.S., Witzke, B.J., Ludvigson, G.A., Brenner, R.L., González, L.A. and **Ravn, R.L.** (2000a) The paleoclimatological significance of Albian (mid-Cretaceous) sphaerosiderites from eastern Saskatchewan and western Manitoba. Summary of Investigations 2000, **Vol. 1**. *Saskatch. Geol. Surv. Misc. Rep.*, **2000-4.1,** 63–75.

White, T.S., Witzke, B.J. and **Ludvigson, G.A.** (2000b) Evidence for an Albian Hudson arm of the North American Cretaceous Western Interior Seaway. *Geol. Soc. Am. Bull.*, **112,** 1342–1355.

White, T.S., Gonzalez, L.A., Ludvigson, G.A. and **Poulsen, C.** (2001) The mid-Cretaceous hydrologic cycle of North America. *Geology*, **29,** 363–366.

Witzke, B.J. and **Ludvigson, G.A.** (1994) The Dakota Formation in Iowa and the type area. In: *Perspectives on the Eastern Margin of the Cretaceous Western Interior Basin* (Eds G.W. Shurr, G.A. Ludvigson and R.H. Hammond), *Geol. Soc. Am. Spec. Paper*, **287,** 43–78.

Witzke, B.J. and **Ludvigson, G.A.** (1996) Coarse-grained eastern facies. In: *Mid-Cretaceous Fluvial Deposits of the Eastern Margin, Western Interior Basin: Nishnabotna Member, Dakota Formation. A Field Guide to the Cretaceous of Guthrie County, North Central GSA Annual Meeting, Ames, Iowa, Field Trip No. 1* (Eds B.J. Witzke and G.A. Ludvigson), *Iowa Geol. Surv. Bur. Guidebook Series*, **17,** 31–38.

Witzke, B.J., Ravn, R.L., Ludvigson, G.A., Joekel, R.M. and **Brenner, R.L.** (1996a) Age correlation of the Nishnabotna Member. In: *Mid-Cretaceous Fluvial Deposits of the Eastern Margin, Western Interior Basin: Nishnabotna Member, Dakota Formation. A Field Guide to the Cretaceous of Guthrie County, North Central GSA Annual Meeting, Ames, Iowa, Field Trip No. 1* (Eds B.J. Witzke and G.A. Ludvigson), *Iowa Geol. Surv. Bur. Guidebook Series*, **17,** 13–18.

Witzke, B.J., Ludvigson, G.A., Brenner, R.A. and **Joekel, R.M.** (1996b) Regional Dakota sedimentation. In: *Mid-Cretaceous Fluvial Deposits of the Eastern Margin, Western Interior Basin: Nishnabotna Member, Dakota Formation. A Field Guide to the Cretaceous of Guthrie County, North Central GSA Annual Meeting, Ames, Iowa, Field Trip No. 1* (Eds B.J. Witzke and G.A. Ludvigson), *Iowa Geol. Surv. Bur. Guidebook Series*, **17,** 7–12.

Young, L.D. (2002) High resolution chemostratigraphic correlations and the development of accommodation space in mid-Cretaceous strata, eastern margin Western Interior Seaway, central United States. Unpubl. MSc Thesis. University of Iowa, Iowa City, IA, 175 pp.

Manuscript received 16 January 2003;
revision accepted 25 August 2003.